Seasonal climate summary southern hemisphere (winter 2003): a warm season with an exceptionally wet August

S.S. Dawkins
National Climate Centre, Bureau of Meteorology, Australia

(Manuscript received March 2004)

Southern hemisphere circulation patterns and associated anomalies for the austral winter 2003 are reviewed, with emphasis given to the Pacific Basin climate indicators and Australian rainfall and temperature patterns.

Some oceanic warming was observed during the middle of the season, associated with the passage of a downwelling Kelvin wave. However by season's end, surface and subsurface ocean temperatures had returned to close to the long-term normals. Overall, observations showed that the El Niño-Southern Oscillation (ENSO) was in a neutral state.

Across Australia, winter 2003 was a season with higher than average temperatures over much of the country. The season as a whole witnessed a return to near average rainfall totals, due mainly to an exceptionally wet August. In fact, 86 per cent of Australia received above median rain for that month.

Introduction

Some oceanic warming was observed during the middle of the season, associated with the passage of a downwelling Kelvin wave. However by season's end, surface and subsurface ocean temperatures had reverted to the long-term normal, while atmospheric indicators such as cloudiness and surface pressure confirmed neutral El Niño-Southern Oscillation (ENSO) conditions.

This summary reviews the southern hemisphere and equatorial climate patterns for winter 2003, with particular attention given to the Australasian and Pacific Regions. The main sources of information for this report are the *Climate Monitoring Bulletin* (Australian Bureau of Meteorology) and the *Climate Diagnostics Bulletin* (Climate Prediction Center, Washington). Further details regarding sources of data are given in the Appendix.

Pacific Basin climate indices

The Troup Southern Oscillation Index*

The sequence of negative Southern Oscillation Index (SOI) values in place at the end of autumn

Corresponding author address: S.S. Dawkins, National Climate Centre, Bureau of Meteorology, GPO Box 1289K, Melbourne, Vic. 3001, Australia.
Email: s.dawkins@bom.gov.au

*The Troup Southern Oscillation Index (SOI) used in this article is ten times the standardised monthly anomaly of the difference in mean sea-level pressure between Tahiti and Darwin. The calculation is based on a sixty-year climatology (1933-1992).

(Beard 2004) continued during June. The SOI value for June was –12.0 (Fig. 1), the last strongly negative value for the 2002/03 El Niño. This very low value was at least in part due to the effects of an active Madden-Julian Oscillation (MJO) event during late May and a subsequent north-east shift of the South Pacific convergence zone (SPCZ), which placed Tahiti directly under the SPCZ. Hence Tahiti pressure values were lower than might have been expected given that few other ENSO indicators supported warm ENSO conditions. The July value of the SOI was +2.9, within one standard deviation of the mean, representing the first positive monthly value since February 2002 (Fawcett and Trewin 2003). The August value of the SOI was –1.8, well within the normal range of values (the index has a standard deviation of 10), and reflected the continued neutral state of the ENSO system. The seasonal average SOI was –3.6.

The June/July and July/August values of the Climate Diagnostics Center Multivariate ENSO Index (MEI) (Wolter and Timlin 1993, 1998) were +0.022 and +0.265 respectively. These values indicated neutral conditions in the equatorial Pacific.

Fig. 1 Southern Oscillation Index, from January 1999 to August 2003. Means and standard deviations used in the computation of the SOI are based on the period 1933-1992.

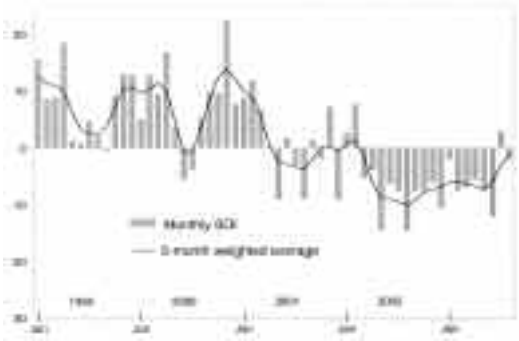

Fig. 2 Standardised anomaly of monthly outgoing long-wave radiation averaged over the area 5ºS to 5ºN and 160ºE to 160ºW, from January 1999 to August 2003. Negative (positive) anomalies indicate enhanced (reduced) convection and rainfall in the area. Anomalies are based on the 1979-1995 base period.

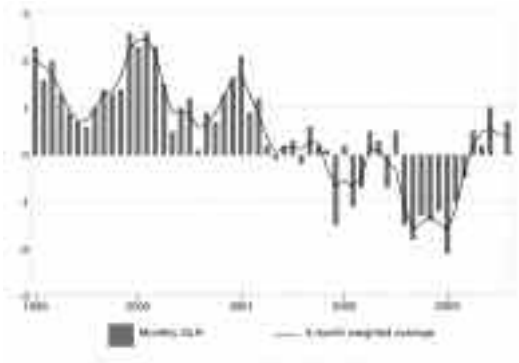

Outgoing long wave radiation

Figure 2, adapted from the Climate Prediction Center (CPC), Washington (CPC 2003), shows the standardised monthly anomaly of outgoing long-wave radiation (OLR) from January 1999 to August 2003, together with a three-month moving average. These data, compiled by the CPC, are a measure of the amount of long wave radiation emitted from an equatorial region centred about the date-line (5ºS to 5ºN and 160ºE to 160ºW). Tropical deep convection in this region is particularly sensitive to changes in the phase of the Southern Oscillation. During warm (El Niño) ENSO events, convection is generally more prevalent resulting in a reduction in OLR. This reduction is due to the lower effective black-body temperature and is associated with increased high cloud and deep convection. The reverse applies in cold (La Niña) events, with less convection expected in the vicinity of the date-line.

The MJO is characterised by waves of enhanced or suppressed convective activity propagating eastward across the Indian Ocean and northern Australian tropics to the western, or sometimes central, Pacific (Wheeler and Weickman 2001). The monthly values –1.0 (June), 0.0 (July) and +0.7 (August) of this index were consistent with a return to a neutral state of the Southern Oscillation. Activity associated with the MJO was minimal during winter.

Oceanic patterns

Sea-surface temperatures

Figure 3 shows winter 2003 sea-surface temperature (SST) anomalies in degrees Celsius (°C), obtained from the NOAA Optimum Interpolation analyses (Reynolds et al. 2002). The contour interval is 0.5°C. Positive anomalies are shown in red shades, while negative anomalies are shown in blue shades.

Fig. 3 Anomalies of sea-surface temperature for winter (June, July, August) 2003. The contour interval is 0.5°C.

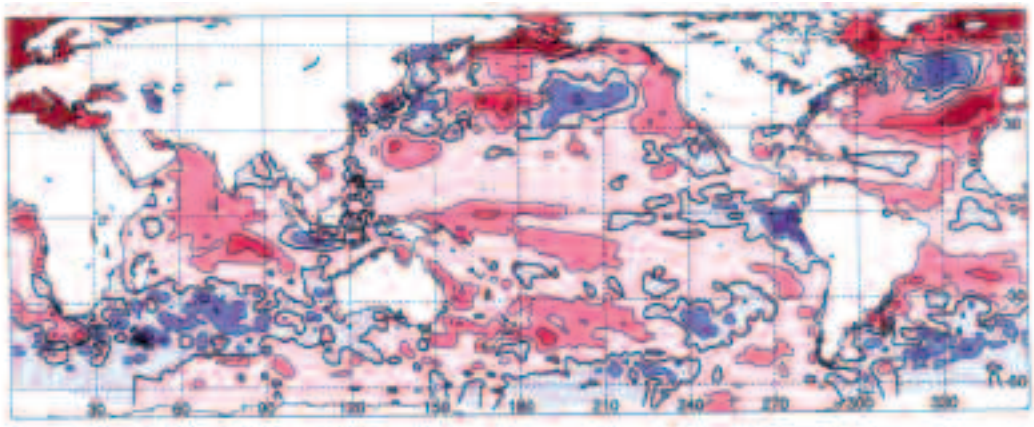

The eastern equatorial cold tongue was stronger than average, with negative anomalies reaching –2°C near the South American coast. Equatorial waters west of the date-line were up to 1°C above the mean for the season. The winter season mean anomalies for NINO3 (eastern equatorial Pacific) and 4 (western equatorial Pacific) were +0.06 and +0.67 respectively, indicating neutral conditions.

In the Indian Ocean, cool SSTs were observed near Java, but a larger area of warm SSTs was present in the central Indian Ocean. This warm/cool pattern of SSTs in the Indian Ocean represents the positive phase of the Indian Ocean Dipole (IOD). A positive phase of the IOD has been associated with below average rainfall over western and southern regions of Australia (Ashok et al. 2003).

Elsewhere, SSTs around Europe were +2°C above average, consistent with the record high land-surface temperatures experienced across that continent.

Subsurface patterns

Figure 4 shows a Hovmöller diagram of the anomaly in metres of the depth of the 20°C isotherm along the equatorial Pacific Ocean between January 1996 and August 2003, as calculated by the Bureau of Meteorology Research Centre (BMRC). This isotherm is generally situated very close to the equatorial ocean thermocline, the region of greatest temperature gradient with respect to depth. The thermocline can also be regarded as the boundary between the upper ocean warm water and the deeper ocean cold water. An abnormally shallow thermocline in the eastern Pacific Ocean is characteristic of La Niña events. Positive anomalies correspond to the 20°C

Fig. 4 Time-longitude section of the monthly anomalous depth of the 20°C isotherm at the equator from January 1996 to August 2003. The contour interval is 10 m.

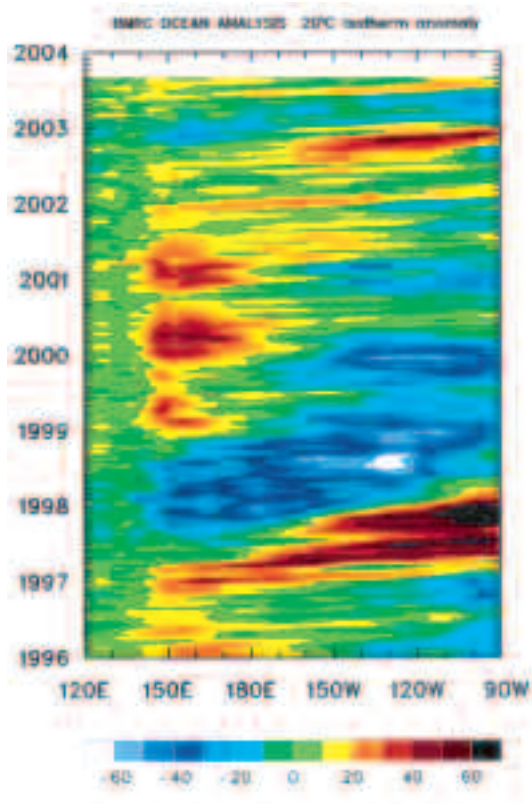

isotherm being deeper than average, and negative anomalies to it being shallower than average.

A downwelling Kelvin wave crossed the Pacific Ocean, starting in the western Pacific in late May/early June traversing to the eastern Pacific by late July. The Kelvin wave produced positive (warm) anomalies in the 20ºC isotherm depth as shown Fig. 4. This oceanic Kelvin wave was triggered by substantial westerly wind anomalies which migrated into the western Pacific during May in association with the MJO. These westerly wind anomalies were the strongest observed for the year, the previous period of equally strong westerly anomalies being in December 2002.

The positive 20ºC isotherm depth anomalies steadily decreased in magnitude from a peak of more than +40 metres near 120°W to less than +20 metres everywhere west of 100°W during July. The August 2003 20ºC isotherm depth anomalies showed values near normal for regions west of 120°W throughout the month. East of 120°W, slightly warm conditions were evident during the first half of the month. However these mostly dissipated by the end of August leaving isotherm depth anomalies generally less than +20 metres. These sightly warm subsurface conditions were the remnants of the downwelling oceanic Kelvin wave that crossed the equatorial Pacific during June.

Figure 5 shows a sequence of equatorial Pacific vertical temperature anomaly profiles for the four months ending August 2003, also obtained from the BMRC. Red (blue) shades in the diagram indicate subsurface waters which are warmer (cooler) than average. These diagrams show the warming of the subsurface associated with the passing of a downwelling Kelvin wave in late May/June and continued associated warming in July. The August subsurface plot shows a return to more average subsurface temperatures, the main feature being the warm water located near the date-line.

Fig. 5 Four-month May to August 2003 sequence of vertical temperature anomalies at the equator for the Pacific Ocean. The contour interval is 0.5°C.

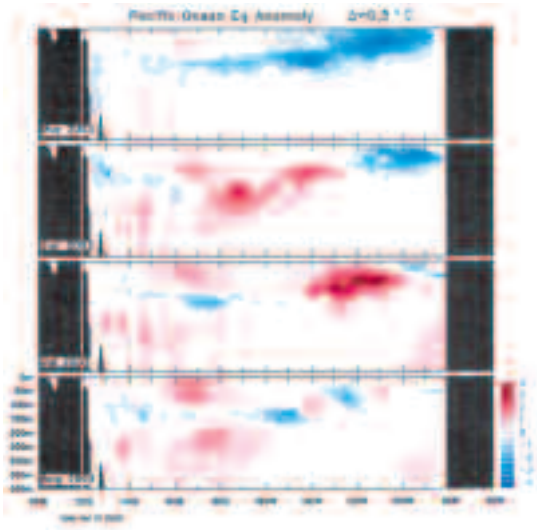

Atmospheric patterns

Surface analyses

The winter 2003 mean sea-level pressure (MSLP) across the southern hemisphere is shown in Fig. 6, with the associated anomalies shown in Fig. 7. These anomalies are the departures from a twenty-two year (1979-2000) climatology obtained from the National Centers for Environmental Prediction (NCEP). The MSLP analysis itself has been computed using data obtained from the Australian Bureau of Meteorology's Global Assimilation and Prediction (GASP) model daily 0000 UTC analyses. The MSLP anomaly field is not shown over areas of elevated topography.

The Antarctic circumpolar trough showed three minima, located at 20°E, 120°E and 130°W. For the most part, the pattern of seasonal mean pressure at high latitudes was close to the climatological average for winter, taking the form of a three wave pattern.

The most noteworthy features of the anomalous MSLP chart (Fig. 7) are the two regions of anomalously high pressure just east of the date-line and near 90°E respectively. These anomalies were associated with blocking episodes in both June and August in both locations. A low pressure anomaly for the season was observed near 90°W, 60°S. An anomalous trough located around 130°E affected south to southeast Australia and was associated with wet conditions in Tasmania.

Mid-tropospheric analyses

The mean 500 hPa geopotential height patterns for winter 2003 are shown in Fig. 8, with anomalies shown in Fig. 9. The characteristics in the MSLP anomaly pattern (Fig. 7) were also present in the 500 hPa anomaly pattern (Fig. 9), with significant troughs (or lows) coinciding with the circumpolar minima in the pressure. There was a region of split flow at the 500 hPa level, just east of the date-line associated with the blocking activity observed in Fig. 7. In the anomaly field, features observed in the surface pressure anomalies are still present, with strong positive anomalies present east of the date-line and also near 90°E. Negative height anomalies were situated over the far southeast Pacific and also to the south and southwest of Tasmania.

Fig. 6 Winter 2003 mean sea-level pressure (hPa). The contour interval is 5 hPa, with values below 990 hPa stippled.

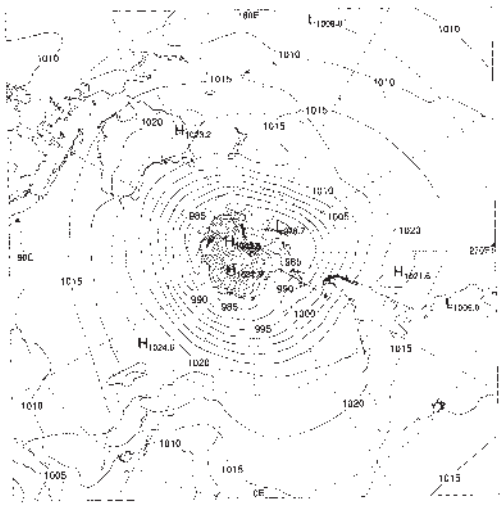

Fig. 7 Winter 2003 mean sea-level pressure anomaly (hPa). The contour interval is 2.5 hPa, with values above 5 hPa and below –5 hPa stippled.

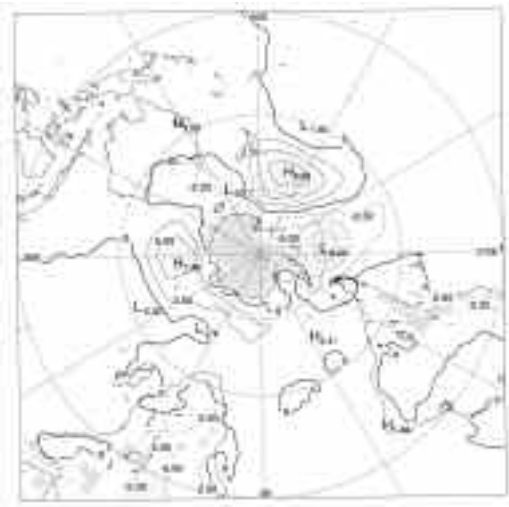

Fig. 8 Winter 2003 500 hPa geopotential height (gpm). The contour interval is 100 gpm.

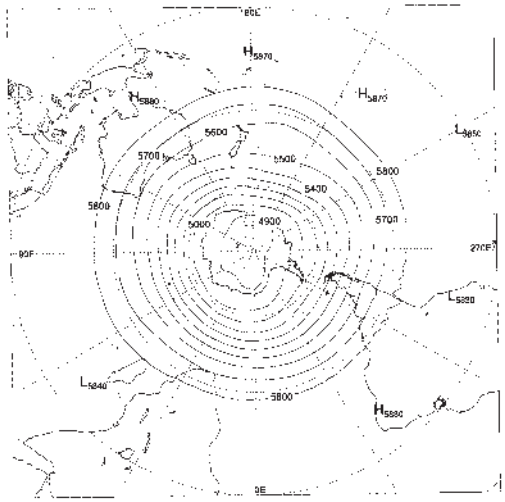

Fig. 9 Winter 2003 500 hPa geopotential height anomaly (gpm). The contour interval is 30 gpm, with values below –90 gpm stippled.

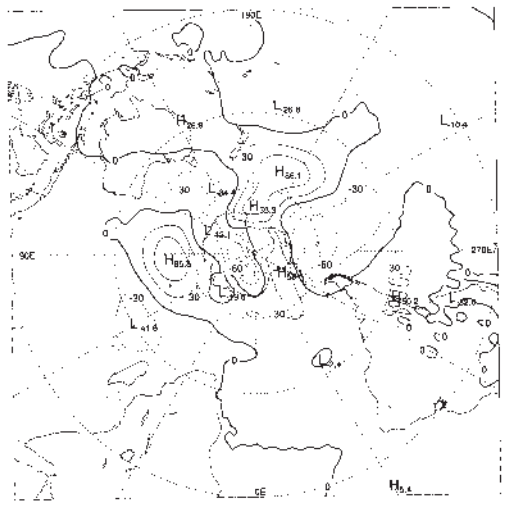

Blocking

Figure 10 is a time-longitude section of the daily southern hemisphere mid-level Blocking Index,

$$BI = 1/2[(u_{25}+u_{30}) - (u_{40}+2u_{45}+u_{50}) + (u_{55}+u_{60})].$$

Here, u_λ indicates the 500 hPa level zonal wind component at λ degrees of southern hemisphere latitude ranging from 0° at the equator to +90°S at the South Pole. The blocking index measures the strength of the 500 hPa flow at the mid-latitudes (40°S to 50°S) relative to that at subtropical (25°S to 30°S) and high (55°S to 60°S) latitudes.

Fig. 10 Winter 2003 daily blocking index (m s^{-1}): time-longitude (Hovmöller) section. The horizontal axis measures degrees of longitude east of the Greenwich meridian. Day one is 1 June 2003.

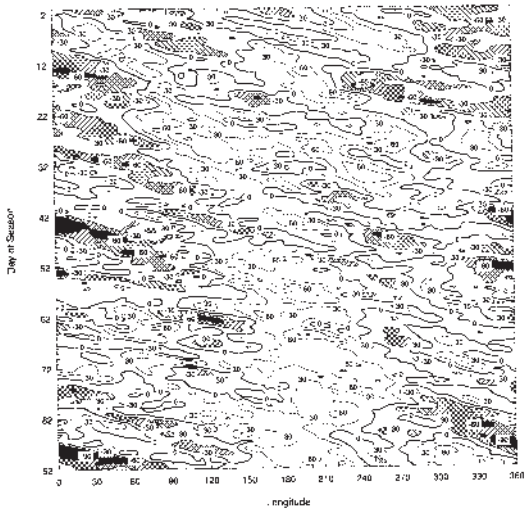

Fig. 11 Mean southern hemisphere blocking index (m s^{-1}) for winter 2003 (solid line). The dashed line shows the corresponding long-term average. The horizontal axis shows degrees east of the Greenwich meridian.

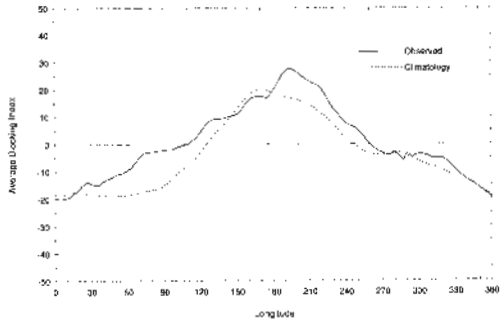

The highest value of the BI for winter was slightly over +90 m s^{-1} near 100°E near the end of June (day 29). Blocking was also present in the Pacific Ocean near 210°E during this time. The most persistent blocking event, centred around 200°E, started mid-July (day 47) and continued throughout the remainder of the season. In contrast, BI values generally remained low in the Atlantic Ocean sector indicating highly mobile zonal flow, as is the climatological norm for this part of the hemisphere.

Taken across the entire season in the form of a seasonal mean (Figure 11), blocking was above average across most of the southern hemisphere, particularly in the Indian and Pacific Ocean sectors. This is consistent with the split upper flow near the date-line at the 500 hPa level, and also with the positive height/pressure anomalies present at both 500 hPa and at mean sea level.

Winds

Low-level (850 hPa) and upper-level (200 hPa) wind anomalies for winter 2003 are shown in Figs 12 and 13 respectively. Isotach contours are at 5 m s^{-1} intervals, and in Fig. 12 the regions of the globe where the land rises above 850 hPa are shaded grey. The low-level pattern in the northern Coral Sea shows a slightly enhanced trade wind regime. East of the date-line, 850 hPa anomalies were generally very small. In other areas, the low-level wind anomalies were consistent with the anomalous MSLP.

Low-level wind anomalies across Australia were mostly weak during winter, the main exception being a band of enhanced westerlies over southeastern Australia. An anticyclonic anomaly was observed in the Coral Sea, a feature consistent with the MSLP and 500 hPa anomalies discussed earlier.

At upper levels the anomaly patterns show enhanced westerly flow to the south of Australia, extending from 110°E to 130°W. Further south in the Southern Ocean/Antarctic area, there is a region of enhanced easterlies extending from 100°E to 150°W. There is also another region of enhanced easterlies off the Queensland coast.

Australian region

Rainfall

Figure 14 shows winter 2003 rainfall totals for Australia. Figure 15 shows the winter rainfall deciles, where the deciles are calculated with respect to gridded rainfall data for all winters from 1900 to 2003.

Winter rainfall was near average across much of the continent. However, above average to very much above average rainfall was recorded over central New South Wales, northern and western Victoria, Tasmania, far north Queensland, Top End of the Northern Territory and in a small patch near Eucla in southern Western Australia. Below average rainfall was observed in a narrow strip along the NSW coastline extending into eastern Victoria, over several isolated patches throughout WA, the Northern Territory, and in central and northern Queensland. Very much below average rainfall was recorded in a band extend-

Fig. 12 Winter 2003 850 hPa vector wind anomalies (m s^{-1}) with contours of vector magnitude overlaid. The contour interval is 5 m s^{-1}, with values above 5 m s^{-1} stippled.

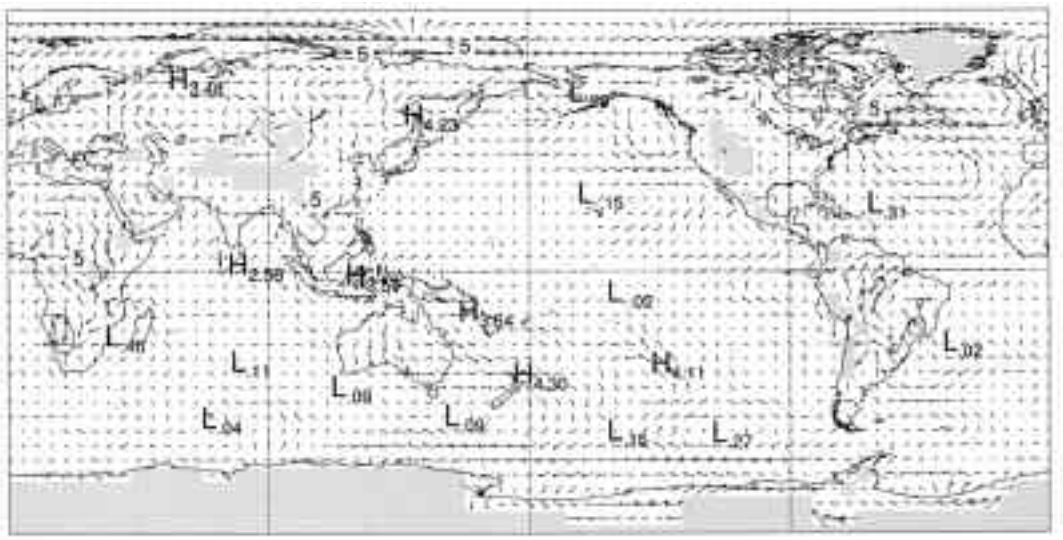

Fig. 13 Winter 2003 200 hPa vector wind anomalies (m s^{-1}) with contours of vector magnitude overlaid. The contour interval is 5 m s^{-1}, with values above 5 m s^{-1} stippled.

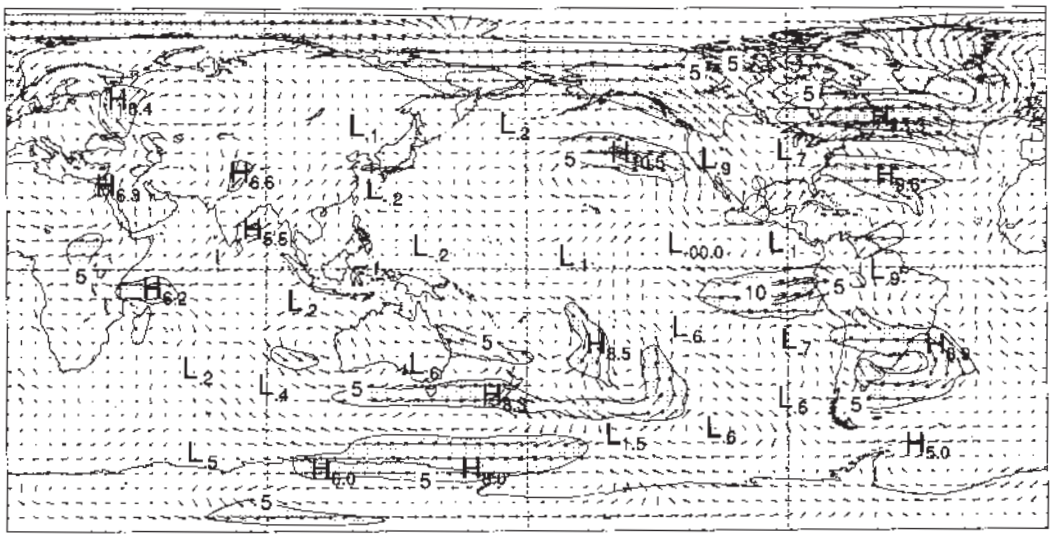

ing from the southern Kimberley to the adjacent central areas of the Northern Territory.

Rainfall in June was close to average across much of Australia. A few regions in southern WA and eastern Victoria recorded very much below to lowest on record totals. Rainfall for July was close to average in most States. A large area in western and central Western Australia recorded below to very much below average rainfall in July. There were substantial regions of below average totals in South Australia, the Northern Territory and Queensland. Above average falls were confined to relatively small areas of southern and southeast Australia, including Tasmania, as well as the far north of the country.

Fig. 14 Winter 2003 rainfall totals for Australia (mm).

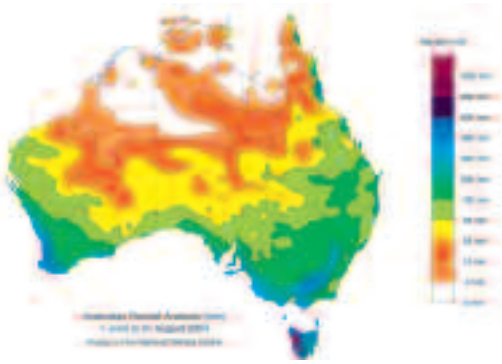

Fig. 15 Winter 2003 rainfall deciles for Australia: decile range values based on grid-point values over the winters 1900 to 2003.

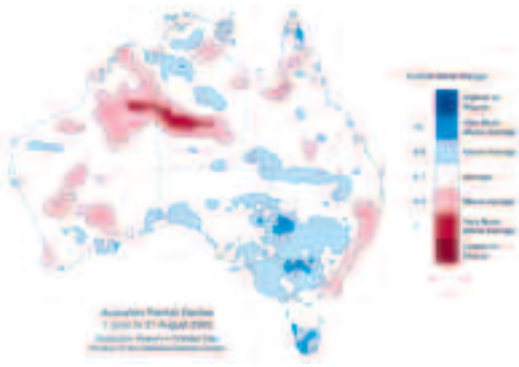

Fig. 16 Winter 2003 maximum temperature anomalies for Australia based on a 1961-1990 mean (°C).

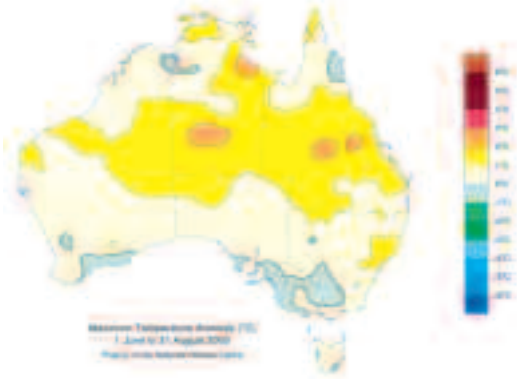

Fig. 17 Winter 2003 minimum temperature anomalies for Australia based on a 1961-1990 mean (°C).

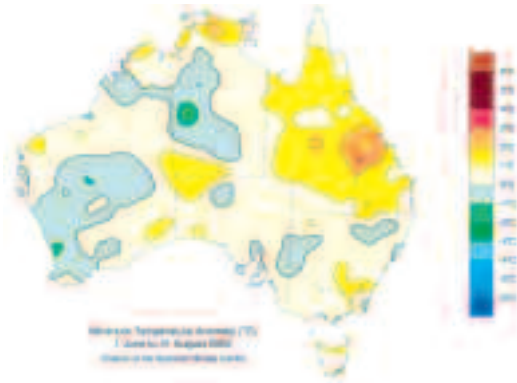

August rainfall in contrast, was well above average across Australia, with all states recording area-averaged rainfall totals in the 8th or 9th decile. In terms of area, 85.9 per cent of the country received above median rainfall, the fourth highest areal coverage for above median August rainfall on record. The wet end to winter removed much of the remaining short-term deficiencies that had developed in the southern half of the continent since March 2003. However, there were still large areas of eastern Australia that were deficient in their twelve-month rainfall totals.

For the six-month period from March to August 2003, the only areas of serious deficiencies that remained were situated in the southern Northern Territory, generally to the north and west of Alice Springs. August rainfall was sufficient to have removed deficiencies near Bairnsdale in Victoria, as well as through parts of central and western South Australia

Table 1 summarises the seasonal rainfall ranks and extremes on a national and State basis.

Temperatures

Maximum and minimum temperature anomalies for winter 2003 are shown in Figs 16 and 17 respectively. The anomalies have been calculated with respect to the 1961-1990 period.

Maximum temperatures were above average for the season across much of the north of the country and

Table 1. Rainfall.

	Highest seasonal total (mm)	*Lowest seasonal total (mm)*	*Highest 24 hour fall (mm)*	*Area-averaged rainfall (AAR) (MM)*	*Rank of AAR**
Australia	1324 at Mount Read (Tasmania)	Zero at several locations (WA, NT, QLD)	190 at Ballina (NSW) on 26th June	63	43
WA	649 at Huntly	Zero at several locations	113 at Cardabia on 26th June	54	41
NT	49 at Wallace Rock Hole	Zero at several locations	37 at Killarney on 17th June	9	54
SA	607 at Piccadilly	7 at Bookabourdie Water Hole	64 at Lake Leake on 6th June	68	68
QLD	949 at Bellenden Ker Top Station	Zero at several locations	118 at Stockdale on 25th June	47	60
NSW	655 at Thredbo Village	37 at South Grafton (Yeerong)	190 at Ballina on 26th June	125	59
VIC	1037 at Rocky Valley	70 at Murray Lock Number 9	111 at Rocky Valley on 24th August	227	81
TAS	1324 at Mount Read	135 at Melton Mowbray	130 at Cornwall on 24th August	493	98

* The rank goes from 1 (lowest) to 104 (highest) and is calculated on the years 1900 to 2003 inclusive.

Table 2. Maximum temperature.

	Highest seasonal mean (°C)	*Lowest seasonal mean (°C)*	*Highest daily recording (°C)*	*Lowest daily recording (°C)*	*Anomaly of area-averaged mean (°C) (AAM)*	*Rank of AAM**
Australia	33.8 at Batchelor (NT)	0.6 at Mt Hotham (Vic)	38.3 at Wyndham (WA) on 31st August	–5.9 at Mount Hotham (Vic) on 2nd June	+0.87	50
WA	33.4 at Kalumburu	14.7 at Rocky Gully	38.3 at Wyndham on 31st August	8.3 at Salmon Gums on 22nd July	+0.65	42
NT	33.8 at Batchelor	20.6 at Kulgera	36.8 at Elliott on 22nd August	14.5 at Arltunga on 16th June and at Kulgera on 23rd July	+1.10	49
SA	21.5 at Marla	8.9 at Mount Lofty	34.1 at Moomba on 12th August	3.4 at Mount Lofty on 10th August	+0.72	40
QLD	32.0 at Weipa	15.4 at Stanthorpe	36.8 at Century Mine on 13th August	8.0 at Stanthorpe on 24th July	+1.27	54
NSW	21.6 at Murwillumbah	2.9 at Charlotte Pass	32.7 at Tibooburra and at Wanaaring on 12th August	–5.0 at Crackenback on 30th August	+0.73	43
VIC	16.4 at Orbost	0.6 at Mt Hotham	25.0 at Swan Hill on 2nd June	–5.9 at Mount Hotham on 2nd June	+0.28	35
TAS	14.7 at Bicheno	3.1 at Mount Wellington	20.4 at Dover on 3rd August	–2.6 at Mount Wellington on 18th and 31st August	+0.61	46

* The temperature ranks go from 1 (lowest) to 54 (highest) and are calculated on the years 1950 to 2003 inclusive.

Table 3. Minimum temperature.

	Highest seasonal mean (°C)	*Lowest seasonal mean (°C)*	*Highest daily recording (°C)*	*Lowest daily recording (°C)*	*Anomaly of area-averaged mean (°C) (AAM)*	*Rank of AAM**
Australia	24.0 at McCluer Island (NT)	–5.4 at Charlotte Pass (NSW)	27.0 at McCluer Island (NT) on 2nd and 4th June	–13.0 at Charlotte Pass (NSW) on 10th and 20th August	+0.54	44
WA	23.3 at Troughton Island	3.8 at Wandering	26.0 at Troughton Island on 9th June	–4.8 at Eyre on 3th July	+0.29	39
NT	24.0 at McCluer Island	4.0 at Arltunga	27.0 at McCluer Island on 2nd and 4th June	–6.0 at Arltunga on 29th July	+0.21	31
SA	10.3 at Cape Willoughby	2.5 at Yongala	17.6 at Moomba on 13th August	–4.8 at Yunta on 20th July	+0.61	42
QLD	23.8 at Coconut Island	2.5 at Stanthorpe	26.0 at Coconut Island on 4th June	–7.1 at Oakey on 28th July	+1.13	48
NSW	12.9 at Byron Bay	–5.4 at Charlotte Pass	20.0 at Byron Bay on 3rd June	–13.0 at Charlotte Pass on 10th and 20th August	+0.57	41
VIC	9.5 at Wilsons Promontory	0.6 at Mt Hotham	15.8 at Point Hicks on 3rd June	–9.3 at Mount Hotham on 20th August	+0.25	34
TAS	9.1 at Swan Island	–1.2 at Mount Wellington	14.9 at Swan Island on 5th June	–2.6 at Mount Wellington on 18th and 31st August	+0.85	4

* The temperature ranks go from 1 (lowest) to 54 (highest) and are calculated on the years 1950 to 2003 inclusive.

within a degree of average over other areas (Fig. 16). In Queensland the State-wide maximum temperature anomaly was +1.27°C, the highest in the post-1950 era. The Australian mean maximum temperature anomaly was +0.87°C above the long-term average, the fifth highest in the post-1950 era.

Winter mean minimum temperatures were above average in Queensland and several smaller regions in other states, whilst elsewhere temperatures were generally within a degree of average. Areas of Queensland near Springsure experienced minimum temperature anomalies of +3 to +4°C for the season. Queensland's State-wide mean minimum temperature anomaly was +1.13°C above the long-term average, the 7th highest in the post-1950 era. In Western Australia temperatures were within a degree of average with the exception of some areas around the Perth metropolitan area that were 1-2°C below average for the season. The seasonal mean minimum temperature anomaly for Australia was +0.54°C.

Mean temperatures were the 6th highest for the country since 1950 with the Australia-wide average anomaly reaching +0.70°C.

Table 2 summarises the seasonal maximum temperature ranks and extremes on a national and State basis, and Table 3 gives the corresponding summary for the seasonal minimum temperatures.

References

Ashok, K., Guan, Z. and Yamagata, T. 2003. Influence of the Indian Ocean Dipole on the Australian winter rainfall. *Geophys. Res. Lett., 30(15)*, 1821, doi:10.1029/2003GL017926.

Australian Bureau of Meteorology. 2003. *Climate Monitoring Bulletin - Australia*, June, July and August 2003 issues. National Climate Centre, Bur. Met., Australia.

Beard, G. 2004. Seasonal climate summary southern hemisphere (autumn 2003): demise of the 2002/03 El Niño event. *Aust. Met. Mag., 53,* 53-63.

Climate Prediction Center. 2003. *Climate Diagnostics Bulletin,* June, July and August 2003 issues. US Department of Commerce,

National Oceanic and Atmospheric Administration, Washington D.C.

Fawcett, R.J.B. and Trewin, B.C. 2003. Seasonal climate summary southern hemisphere (autumn 2002): onset of El Niño conditions. *Aust. Met. Mag., 52*, 127-36.

Reynolds, R.W., Rayner, N.A., Smith, T.M., Stokes, D.C. and Wang, W. 2002. An improved in situ and satellite SST analysis for climate. *Jnl climate, 15*, 1609-25.

Wheeler, M. and Weickmann, K.M. 2001. Real-time monitoring and prediction of modes of coherent synoptic to intraseasonal tropical variability. *Mon. Weath. Rev., 129*, 2677-94.

Wolter, K. and Timlin, M.S. 1993. Monitoring ENSO in COADS with a seasonally adjusted principal component index. *Proc. of the 17th Climate Diagnostics Workshop*, Norman, OK, NOAA/NMC/CAC, NSSL, Oklahoma Clim. Survey, CIMMS and the School of Meteor., Univ. of Oklahoma, 52-57.

Wolter, K. and Timlin, M.S. 1998. Measuring the strength of ENSO - how does 1997/98 rank? *Weather, 53,* 315-24.

Appendix

Data sources used for this review were:

- National Climate Centre, *Climate Monitoring Bulletin - Australia*. Obtainable from the National Climate Centre, Australian Bureau of Meteorology, GPO Box 1289K, Melbourne, Vic. 3001, Australia.

- Climate Prediction Center (CPC), *Climate Diagnostics Bulletin*. Obtainable from the Climate Prediction Center (CPC), National Weather Service, Washington D.C., 20233, USA.